Poultry Science®

Bacteriophage LHE83 targeting OmpA as a receptor exhibited synergism with spectinomycin against *Escherichia coli*

Jianyu Zhen,[*,1] Rui Liu,[*,1] Cheng Man,[*] Shijie Xu,[*] Wenxiu Zhang,[*] Ling Zou,[*] Wenhua Liu,[*] Hong-Bo Ni,[*] Ming Zou,[*] Tao He,[†] Ran Wang,[†] Xiao-Xuan Zhang,[*] and Can Zhang [*,2]

[*]*College of Veterinary Medicine, Qingdao Agricultural University, Qingdao, China; and* [†]*Institute of Food Safety and Nutrition, Jiangsu Academy of Agricultural Sciences, Nanjing, China*

ABSTRACT Understanding the characteristics of bacteriophages is crucial for the optimization of phage therapy. In this study, the biological and genomic characteristics of coliphage LHE83 were determined and its synergistic effects with different types of antibiotics against *E. coli* E82 were investigated. Phage LHE83 displayed a contractile tail morphology and had a titer of 3.02×10^9 pfu/mL at an optimal MOI of 0.01. Meanwhile, phage LHE83 exhibited good physical and chemical factors tolerance. The 1-step growth analysis revealed a latent period of approx. 10 min with a burst size of 87 pfu/infected cell. Phage LHE83 belongs to the genus *Dhakavirus*. Its genome consists of 170,464 bp with a 40% GC content, and a total of 268 Open Reading Frames (**ORF**) were predicted with no detected virulent or resistant genes. *ORF 213* was predicted to encode the receptor binding protein (**RBP**) and confirmed by the antibody-blocking assay. Furthermore, a phage-resistant strain *E. coli* E82R was generated by co-culturing phage LHE83 with *E. coli* E82. Genomic analysis revealed that OmpA served as the receptor for phage LHE83, which was further confirmed by phage adsorption assay using *E. coli* BL21ΔOmpA, *E. coli* BL21ΔOmpA: OmpA and *E. coli* BL21:OmpA strains. Additionally, a synergistic effect was observed between phage LHE83 and spectinomycin against the drug-resistant strain *E. coli* E82. These results provide a theoretical basis for understanding the interactions between phages, antibiotics, and host bacteria, which can assist in the clinical application of phages and antibiotics against drug-resistant bacteria.

Key words: bacteriophage, receptor binding protein, OmpA, spectinomycin, synergistic effect

2024 Poultry Science 103:103643
https://doi.org/10.1016/j.psj.2024.103643

INTRODUCTION

Pathogenic *Escherichia coli*, as an opportunistic pathogen and commensal bacterium, widely exists in the environment and the intestines of animals. It is responsible for intestinal infections, peritonitis, and colisepticemia, posing significant challenges to animal production worldwide. Antibiotics have traditionally been used for the treatment of colibacillosis. However, the improper and excessive use of antibiotics has resulted in antibiotic residue and the emergence of multidrug-resistant strains (Monroe S, 2000; Ajiboye, et al., 2009). Therefore, there is an urgent need to explore alternative substitutes for antibiotics (von Baum and Marre, 2005).

Bacteriophages are increasingly recognized as viable alternatives to antibiotics in the prevention and treatment of bacterial infections, particularly those caused by drug-resistant strains (Clokie, et al., 2011; Gordillo Altamirano and Barr, 2019; Strathdee, et al., 2023). Phages could specifically adsorb to their bacterial host surface through receptor binding proteins (**RBP**), initiating the lysis process with high host specificity(Lavelle, et al., 2020; Taslem Mourosi, et al., 2022). However, this specificity limits their lytic spectrum in clinical applications. Combining multiple phages in a cocktail is a common approach to enhance successful infection and lysis, ultimately improving the overall efficacy of phages. However, The design of a phage cocktail should focus on specific phage selection through a rational and evidence-based approach (Jin, et al., 2023).

It is currently believed that RBP at the tip of the phage tail fibers plays a key role in host receptor recognition (Gonzalez-Serrano, et al., 2020; Taslem Mourosie et al., 2022; Degroux, et al., 2023). Phages can target various bacterial surface elements, such as peptidoglycan and teichoic acids, glycolipid moieties,

Received January 26, 2024.
Accepted March 7, 2024.

[1]These authors contributed equally to this work.

[2]Corresponding author. cleverflame@163.com

polysaccharide components, membrane proteins, pili, and flagella (Ofir and Sorek, 2018). During the long co-evolutionary process between phages and bacteria, the most common adaptation of host bacteria is to alter their receptors (Labrie, et al., 2010), which leads to rapid resistance development (Oechslin, 2018). The importance of bacterial surface receptors is so crucial that phage infection simply cannot take place without them. Therefore, the combination of phage cocktails targeting different receptors could reduce resistance likelihood and antagonism. Thus, understanding the phage-host interaction is vital for developing effective phage cocktails (Gordillo Altamirano and Barr, 2021).

It is reported that the combination of phages with antibiotics can produce synergistic effects, effectively increasing the susceptibility of bacterial strains to drugs and promoting the generation of progeny phages (North and Brown, 2021). The synergistic interaction between bacteriophages and antibiotics is attributed to various mechanisms, such as modulation of bacterial metabolism and replication, activation of the immune response, and destabilization of bacterial biofilm. For instance, OmpA, a potential receptor for bacteriophages, plays a crucial role in the resistance of *A. baumannii* to chloramphenicol, aztreonam, and nalidixic acid(Smani, et al., 2014). These synergistic effects significantly enhance the bacterial susceptibility to antibiotics (Wang, et al., 2021; Zuo, et al., 2021). However, the specific synergy mechanism between phages and various antibiotics has not been fully elucidated, highlighting the need for further exploration of unexplored phage-antibiotic combinations.

In this study, a novel phage LHE83 was isolated and identified, its RBP was characterized, and the specific receptors on the host cell surface recognized by RBP were identified. Additionally, the synergy effects of phage LHE83 in combination with Spectinomycin against *E. coli* E82 were assessed. These findings provided valuable insights for the development of phage cocktails based on receptor recognition, which can enhance the effectiveness of phage therapy against particular bacterial strains.

RESULTS

Characteristic Analysis of Bacteriophage LHE83

Isolation and Morphology of Phage LHE83. A novel virulent phage LHE83 was isolated from broiler feces using the double layer method. LHE83 formed a clear plaque (size: 1.5 ± 0.5 mm in diameter) on the lawn of *E. coli* E82 (Figure 1A). The transmission electron microscope (TEM) morphology showed that phage LHE83 had a regular icosahedral head (approximately 110 nm in diameter) and a contractile sheathed tail (approximately 100 nm in length) (Figure 1B).

Biological Characterization of Phage LHE83. The host range of LHE83 was tested on 96 *E. coli* isolates, and it was effective against 19.8% (19/96) of them, including various serotypes such as O55, O78, O111, O114, O119, O125, and O127a. Notably, the proliferation efficiency of phage LHE83 varied significantly among the 19 host strains, with the efficiency of plating (EOP) ranging from 10^6 to 10^9 pfu/mL (Table 1). Phage LHE83 had the highest titer of 3.02×10^9 pfu/mL on the *E. coli* E82 strain at an optimal MOI of 0. 01.

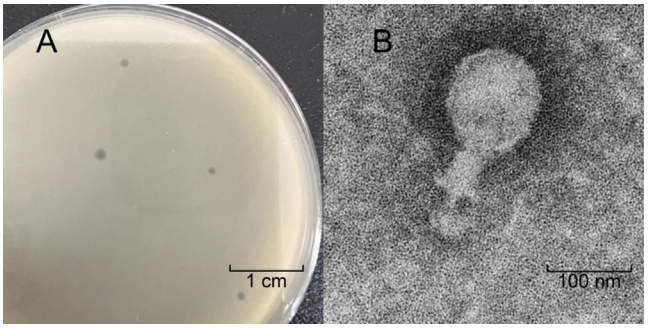

Figure 1. Morphology of phage LHE83. (A) Phage plaques formed on double-layered agar plates. (B) Morphology of phage LHE83 in TEM (magnification: × 70.0 K).

The tolerance of phage LHE83 to various physical and chemical factors was examined. It showed that LHE83 had good resistance to ultraviolet radiation, with a 3-log decrease in titer after 1 h of exposure (Figure 2A). It was kept stable at 40° to 50°C (Figure 2B), as well as within the range of pH 4 to 10 (Figure 2C). The one-step growth analysis of phage LHE83 showed a latent period of approximately 10 min, followed by a rapid increase in the number of released viral particles. It took about 40 min to reach the growth plateau phase, with a burst size of 87 pfu/infected cell (Fig 2D).

Genomic Characterization of Phage LHE83. The phage LHE83 genome was sequenced and submitted to GenBank Direct Submission (National Center of Biotechnology Information, NCBI) nucleotide sequence database and has been assigned the accession number OQ561750. Its genome revealed a 170,464 bp length with a 40% GC content. Genome annotation predicated 268 *ORF*, 227 of which were identified as positive-stranded and 76 as negative-stranded. Further annotation identified 120 functional genes, which play important roles in various biological processes. There were 37 structure-related genes, 3 lysis-related genes, and 78 genes associated with transcription and replication. Additionally, 2 tRNAs were predicted, while no virulence or drug-resistance genes were found in the genome (Figure 3). The genome sequence of phage LHE83 was blasted with the GeneBank database, and an evolutionary tree was constructed using MEGA software (Figure 4). The homology analysis revealed an 80.99% ~ 98.00% similarity between phage LHE83 and 10 other phages. According to the current guidelines of the International Committee on Taxonomy of Viruses (**ICTV**), all of these phages belong to the family *Straboviridae* and the genus *Dhakavirus*. Additionally, due to the high homology between phage LHE83 and our previously reported phage Bp7, a genomic collinearity analysis was conducted on them, indicating the absence of large-scale

Table 1. The host ranges of phage LHE83 and phage Bp7.

Strain name	Serotype	Bp7	EOP for LHE83
E4	O55: K59	-	0.026
E8	O114: K90	-	0.025
E10	O119: K69	-	0.078
E12	—	-	0.003
E14	O127a: K63	+	0.031
E28	O55: K59	+	0.010
E29	O78: K80	+	0.009
E30	O78: K80	+	0.007
E48	O142: K86	+	-
E53	O78: K80	-	0.002
E56	025: K19	+	-
E58	O111: K58	+	0.005
E61	O119: K69	-	0.008
E63	O15	+	-
E71	O111: K58	-	0.010
E74	O125: K70	-	0.002
E81	O78: K80	+	0.223
E82	O78: K80	-	1
E83	O8	+	0.417
E85	—	-	0.252
E90	—	+	0.221
E91	O78: K80	+	-
E93	—	+	0.202
E1	O78: K80 (B)	-	-
E2	O125: K70 (B15)	-	-
E3	025: K19 (L)	-	-
E5	O15	-	-
E6	O125: K70 (B15)	-	-
E7	O78: K80 (B)	-	-
E9	O78: K80 (B)	-	-
E11	O14: K90 (B)	-	-
E13	O8: K40 (A), K47 (A)	-	-
E15	O8	-	-
E16	O25: K19 (L)	-	-
E17	O25: K19 (L)	-	-
E18	O15	-	-
E19	O111: K58 (B4)	-	-
E20	O142: K86 (B)	-	-
E21	O128: K67 (B12)	-	-
E22	O6: K15	-	-
E23	O125: K70 (B15)	-	-
E24	O125: K70 (B15)	-	-
E25	O114: K90 (B)	-	-
E26	O7: K1 (L)	-	-
E27	O143	-	-
E31	O29	-	-
E32	O78:K80 (B)	-	-
E33	O78: K80 (B)	-	-
E34	O20: K17 (L)	-	-
E35	—	-	-
E36	—	-	-
E37	O111: K58 (B4)	-	-
E38	O128: K67 (B12)	-	-
E39	—	-	-
E40	O86: K61 (B7)	-	-
E41	O114: K90 (B)	-	-
E42	O136: K78	-	-
E43	O55: K59 (B5)	-	-
E44	O44: K7 (L)	-	-
E45	O114: K90 (B)	-	-
E46	O125: K70 (B15)	-	-
E47	O7: K1 (L)	-	-
E49	O15	-	-
E50	O55: K59 (B5)	-	-
E51	O25: K19 (L)	-	-
E52	O78: K80(B), O55: K59 (B5)	-	-
E54	O78: K80 (B)	-	-
E55	—	-	-
E57	0114: K90 (B)	-	-
E59	O111: K58 (B4)	-	-
E60	O7: K1 (L)	-	-
E62	O86: K61 (B7)	-	-
E64	O78: K80 (B)	-	-
E65	O55: K59 (B5)	-	-
E66	O111: K58 (B4)	-	-
E67	O7: K1 (L)	-	-
E68	O6: K15	-	-
E69	O78: K80 (B)	-	-
E70	O125: K70 (B15)	-	-
E72	O8	-	-
E73	O86: K61 (B7)	-	-
E75	O111: K58 (84)	-	-
E76	O8	-	-
E77	—	-	-
E78	O78: K80 (B)	-	-
E79	—	-	-
E80	O78: K80 (B)	-	-
E84	O78: K80 (B)	-	-
E86	O26	-	-
E87	O26	-	-
E88	O78: K80 (B)	-	-
E89	—	-	-
E92	O26	-	-
E94	—	-	-
E95	O78: K80 (B)	-	-
E96	O4	-	-

(*continued*)

sequence recombination, with a high degree of homology observed in most genes (Figure S1). However, the homology of tail fiber genes associated with the phage adsorption was notably low, which may be attributed to the different host spectra between phage LHE83 and phage Bp7 (Table 1).

Identification of RBP of Phage LHE83

The RBP at the tip of long tail fibers serves as the primary functional and structural units of T-even phages during the adsorption process. They also determine phage host specificity, such as gene product 37 (**GP37**) or GP38 in the T4 superfamily (Trojet et al., 2011). To identify the RBP of phage LHE83, the predicted tail fiber GP213, encoding by *ORF 213* of phage LHE83, was compared with GP38 of phage Bp7, which is known as the RBP of phage Bp7 (Chen et al., 2020). The analysis revealed a high homology at the N-terminal region but a low homology at the C-terminal region between GP213 of phage LHE83 and the RBP of phage Bp7 (Figure S2). Furthermore, the C-terminal sequence of GP213 exhibited typical mosaic features, which is consistent with a previous report (Trojet et al., 2011). Based on these findings, it is predicted that GP213 also serves as the RBP of phage LHE83. To further explore whether GP213 is involved in the process of phage adsorption of host bacteria, *ORF 213* was expressed in *E. coli* BL21 (Figure S3). Subsequently, the rabbit antiserum against GP213 was generated after 3 immunizations and used for the antibody-blocking assay. The efficiency of the GP213 antiserum in blocking phage LHE83 adsorption was tested on *E. coli* E82 (Figure 5A). The results showed that the antiserum of GP213 completely blocked phage adsorption, indicating that GP213 indeed serves as the RBP phage LHE83, and plays an important role in the adsorption process.

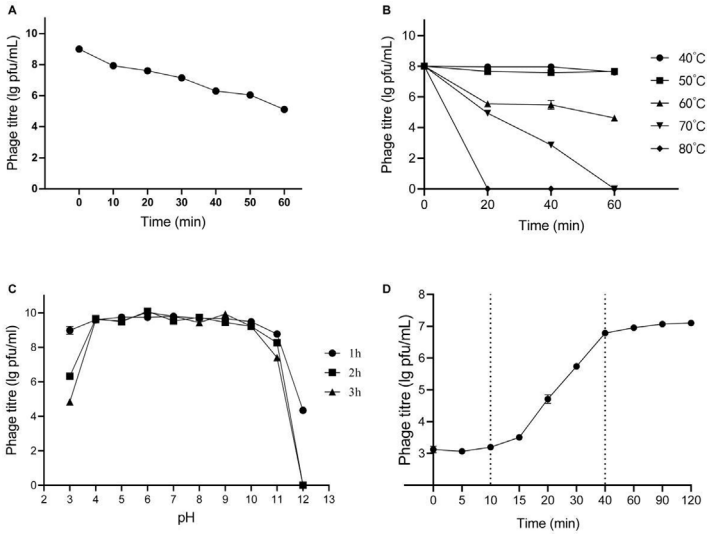

Figure 2. Biological characterization of phage LHE83. (A) UV stability. (B) Thermal stability. (C) pH stability. (D) One-step growth curve on *E. coli* E82. All the data are shown as the mean ± SD.

Identification of Receptor Targeted by Phage LHE83

Resistant strain *E. coli* E82-R5 was isolated from a co-cultured system of phage LHE83 and *E. coli* E82. To understand the genetic changes responsible for resistance development, the genomes of *E. coli* E82 and *E. coli* E82-R5 were sequenced and compared. The analysis revealed that in the genome of *E. coli* E82-R5, there were 5 additional base insertions at the 394th base position of *ORF OmpA*. This insertion caused a frameshift mutation within the *ORF OmpA*, resulting in an altered reading frame and premature termination of OmpA translation. So it is predicted the OmpA serves as the receptor targeted by phage LHE83. To further verify the role of OmpA in phage LHE83 infection, the mutant strain *E. coli* BL21 ΔOmpA was constructed using the scarless Cas9-assisted recombineering (no-SCAR) system to assay the phage adsorption rate changes. The results showed that *E. coli* BL21 ΔOmpA caused an approx. 50% decrease in phage adsorption rate compared to the wild-type strain. Conversely, the complementary strain *E. coli* BL21ΔOmpA: OmpA exhibited approx.90% phage binding activity compared to the wild-type strain. Moreover, the overexpression of OmpA in *E. coli* BL21: OmpA strain led to an approx.120% increase in phage adsorption rate (Figure 5B). These findings confirmed that OmpA was the receptor recognized by phage LHE83 and played a crucial role in the phage adsorption process.

Synergistic Inhibition of E. coli *E82 by Phage LHE83 and Spectinomycin*

It is reported that phage and antibiotics had synergistic effects on the resistant bacterial strains (Allen, et al., 2017).

A checkerboard assay was conducted by combining serially diluted phage LHE83 and different antibiotics on the drug-resistant strain *E. coli* E82, including Neomycin (**NEO**), Doxycycline (**DOX**), Colistin (**COL**), Amoxicillin (**AMX**), Enrofloxacin (**ENR**) and spectinomycin (**SPEC**). The antimicrobial effects were measured for 12 h with 1 h intervals. The results indicated

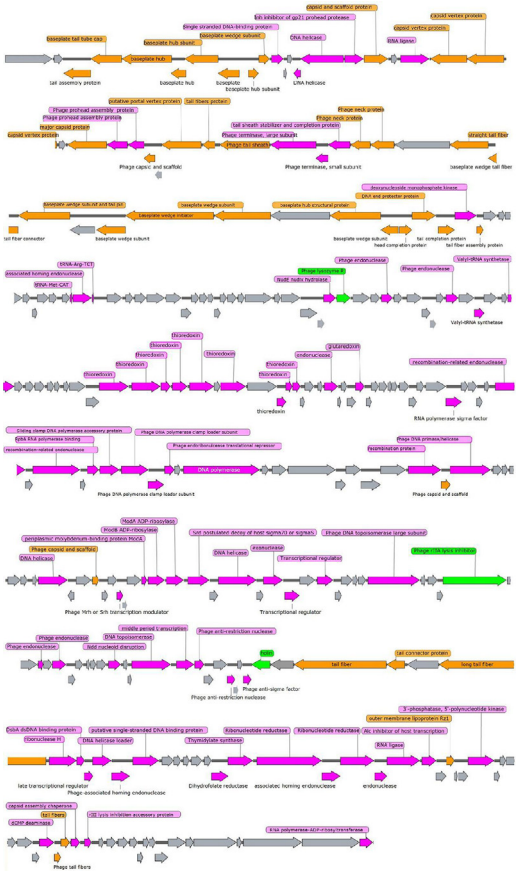

Figure 3. Genome annotation of phage LHE83. The arrows indicate the direction of transcription of each gene. The colors represent *ORF* with different predictive functions: the structural and packaging proteins are marked with orange, the lysis-related proteins are marked with green, the proteins associated with transcriptional regulation are marked with pink, and the hypothetical proteins are marked with grey.

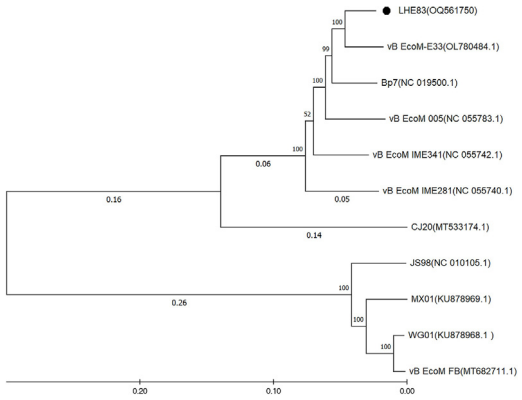

Figure 4. The evolutionary tree of phage LHE83. A total of 10 orthologous phages were selected for the phylogenetic analysis. The evolutionary tree is constructed based on the whole genome using the neighbor-joining method with the default parameter in MEGA software. Reliability values are shown above branches, while evolutionary distances are shown below branches. Distances less than 0.05 were hidden for clarity. • Represents phage LHE83.

that phage LHE83 had no apparent interaction with NEO/AMX, had an antagonistic effect with DOX, and had a slight synergic effect with COL/ENR (Figure S4). A significant synergy was observed between phage LHE83 and SPEC (Figure 6).

The *E. coli* E82 showed no growth inhibition when treated with SPEC alone at concentrations ranging from 0.5 to 32 μg/mL. Treatment with phage LHE83 at a concentration of 10^9 pfu/mL led to significant growth inhibition within 6 h (Figure 6A). However, resistant bacteria rapidly emerged within 10 h (Figure 6B). Compared to the groups treated with SPEC and phage LHE83 alone, the combination of them exhibited significant synergistic effects. The addition of phage LHE83 at a concentration of 10^8 pfu/mL significantly inhibited the growth of *E. coli* E82 with different concentrations of SPEC, even at the lowest concentration of 0.5 μg/mL, a noticeable bacteriostatic effect was observed and maintained for at least 12 h (Figure 6B).

DISCUSSION

Phages efficiently infect host bacteria and maintain a dynamic balance with host bacteria through evolution. In response, bacteria have developed various defense mechanisms against phages, such as restriction modification, CRISPR−Cas adaptive immunity, quorum-sensing system, and receptor mutations. Among these strategies, receptor modifications on the cell surface are the most common defense strategies employed by bacteria to prevent phage adsorption (Hoyland-Kroghsbo, et al., 2013; Diaz-Munoz and Koskella, 2014; Tan et al., 2015; Hampton et al., 2020). The initial stage of phage infection is to specifically adsorb receptors on the surface of the bacteria. Structural alterations or loss of these surface receptors can result in the inability of phages to successfully adsorb to the bacterial surface (Li, et al., 2018). Gene loss, inversion, insertion, and other genetic changes can also affect receptor coding genes, such as MutL-mediated loss of genomic fragments in *P. aeruginosa*, resulting in O-antigen deletion and prevention of phage adsorption (Shen, et al., 2018). Identification of RBP

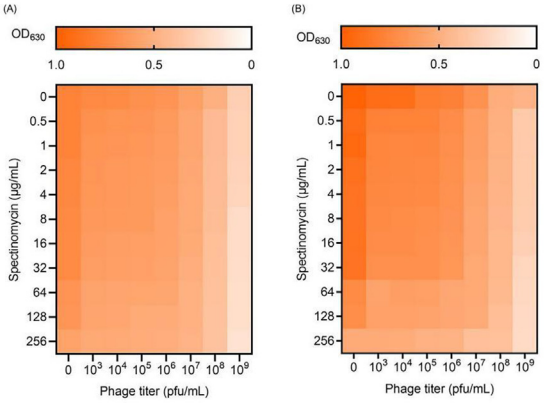

Figure 6. Synergistic effects between phage LHE83 and SPEC against the *E. coli* E82. The co-effect of phage LHE83 and SPEC in different concentrations on *E. coli* E82 after (A) 6 h and (B) 12 h of treatment.

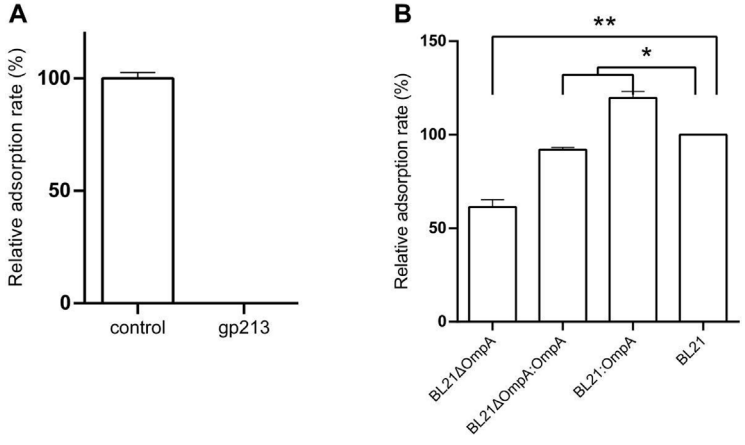

Figure 5. The RBP of phage LHE83 and its recognized receptor identification. (A) The antiserum of GP213 completely blocked the adsorption and infection of phage LHE83 to *E. coli* E82. A negative serum collected before immunization was used as a control. (B) The phage LHE83 adsorption rates on the knockout strain *E. coli* BL21ΔOmpA, the complementary strain *E. coli* BL21ΔOmpA: OmpA, and the overexpression strain *E. coli* BL21:OmpA. All assays were performed in triplicate.

and their receptors in isolated phages is crucial for developing phage cocktails targeting different receptors and expanding the host range. Additionally, it facilitates the expansion of the host range through phage engineering. In this study, phage LHE83 was isolated and characterized, and its RBP and the corresponding receptor on the host cell surface were successfully identified.

Based on homology analysis with the GenBank database, Phage LHE83 showed a high homology with phage Bp7, which belongs to the T-even like phage with GP38 as its RBP (Chen et al., 2020). The RBP of T-even-like phages is typically encoded by genes *GP37* or *GP38*, and had a common feature that highly conserved glycine-rich motifs (**GRM**) were interval by highly variable segments (**HVS**) and showed a mosaic character (Trojet et al., 2011). GP213 of phage LHE83 also showed a similar character. Therefore, it is speculated that GP213 serves as the RBP of phage LHE83. As anticipated, the antibody-blocking assay provided further confirmation that the antiserum of GP213 could completely inhibit the adsorption of phage LHE83 to host bacteria.

Additionally, the genome sequence of phage LHE83-resistant mutant *E. coli* E82R5 revealed that OmpA served as the receptor of phage LHE83. However, the strain *E. coli* E82R5 had a multidrug-resistant phenotype, so the gene knockout and complement experiments of OmpA were performed on engineered bacteria strain *E. coli* BL21. Interestingly, the *E. coli* BL21ΔOmpA strain remained susceptible to phage LHE83 with a 50% reduction in absorption rate. Therefore, although the OmpA mutation of *E. coli* E82 could be completely resistant to phage LHE83, there should be additional receptors on the surface of *E. coli* BL21 recognized by phage LHE83 and need for further investigation.

There were high similarities in the genome and biological characteristics between LHE83 and Bp7, indicating a close relationship between them. Furthermore, their host spectrum was highly overlapped (Table 1). Both phage LHE83 and Bp7 can infect various serotypes of *E. coli*, but their host spectrum is inconsistent, primarily due to their RBP. The N-terminal sequence of GP213 shows a high similarity to that of GP38, and their C-terminal region exhibits similar GRM domains (Fig S2). The main difference lies in the HVS regions in their C-terminal sequence. This suggests that the HVS regions are involved in receptor recognition, which determines whether phage Bp7 and LHE83 recognize receptors LamB and OmpC or OmpA on the host surface, thereby affecting the host spectrum. Therefore, the host spectrum of phages can be expanded by modifying the HVS regions of RBP through genetic engineering techniques, potentially enhancing their antibacterial efficacy.

As a therapeutic agent, phage is not influenced by the drug-resistance mechanisms of bacteria for its unique receptor-recognized infection process (Elbreki, et al., 2014). It was reported that phages can effectively inhibit the growth of drug-resistant bacteria and the formation of bacterial biofilm, thereby enhancing the efficacy of antibiotic therapy (Chaudhry et al., 2017; Aghaee et al., 2021; Li et al., 2021; Simon et al., 2021). Although some antibiotics exhibited antagonistic effects against phages, the overall benefits of combining the phage and antibiotics outweigh the disadvantages (Torres-Barcelo et al., 2018). Phage LHE83 exhibited diverse interactions with various antibiotics on *E. coli* E82, ranging from synergistic to uncorrelated or antagonistic effects. Phage LHE83 showed an obvious synergism with SPEC. Furthermore, the combination treatment exhibited a longer bacteriostatic effect compared to using the phage alone. These findings offer a promising strategy for combating antibiotic-resistant bacteria.

Bacteria have developed complex mechanisms to confer strong resistance to antibiotics, such as the modification in cell membrane permeability, production of aminoglycoside-modifying enzymes, alteration in drug targets on ribosomes, and acquisition/activation of multidrug efflux pump (Gao et al., 2022; Zhang et al., 2023). Our investigation indicated a synergy mechanism between SPEC and phage. SPEC is hypothesized to act on the 30S subunit of bacterial ribosomes, subsequently interfering with bacterial protein synthesis and increasing bacterial susceptibility to phage infection. Further research is needed to elucidate the specific mechanisms underlying the synergy between SPEC and phage LHE83, providing more effective treatment strategies against antibiotic resistance.

CONCLUSIONS

In this study, a phage LHE83 with a well potential application value was characterized, which absorbed the OmpA receptor of host bacteria through its RBP GP213. SPEC had a synergistic effect with LHE83, even at a very low concentration. These findings will contribute to the future clinical application of phage LHE83.

MATERIALS AND METHODS

Description of Bacterial Strains and Culture Conditions

A total of 96 clinical pathogenic *E. coli*, isolated from the broiler farm in Shandong Province, China, were used to test the host range of the phage (Table 1). *E. coli* BL21 (DE3) strain was kept in our lab. All of the bacterial strains were cultured to logarithmic growth phase in Luria-Bertani (**LB**) medium at 37°C and stored at 4°C until used. Neomycin, doxycycline, colistin, amoxicillin, enrofloxacin and spectinomycin were purchased from Macklin (Shanghai Macklin Biochemical Co., Ltd., Shanghai, China).

Phage Isolation

The feces samples were collected from broiler farms in Shandong Province to isolate phages using the previously described method (Zhang et al., 2013). In brief, *E. coli* E82 was used to enrich phages in the sample extract, followed by the isolation and purification of phages using

the double layer agar plate method. The isolated phage was named LHE83 and stored as 30% glycerol stocks at −80°C until used.

Electron Microscope Observation of Phage LHE83

The morphology of phage LHE83 was observed by transmission electron microscopy (TEM, HT7700, Hitachi, Japan). Briefly, 10 μL suspension (10^9 pfu/mL) was dropped onto a copper grid and incubated for 10 min at room temperature, the grid was then stained with 2% phosphotungstic acid (**PTA**) for 5 min. After air drying, the phages on the grid were observed by TEM.

Host Range and EOP of Phage LHE83

The host range and EOP of phage LHE83 were evaluated by the standard double-layer agar plate method as described before (Sui et al., 2021). The EOP of phage LHE83 on the *E. coli* E82 strain was set as 1, and the EOP on other host strains was determined by comparing the phage titer on those strains to that on *E. coli* E82.

Optimal MOI for Phage LHE83 Production

The optimal multiplicity of infection (**MOI**) of phage LHE83 was determined by double-layer agar plate method. In brief, diluted phage LHE83 (10^3−10^9 pfu/mL) and *E. coli* E82 (10^7 cfu/mL) were co-cultured in LB liquid medium at 37°C for 4 h. A culture of *E. coli* E82 (10^7 cfu/mL) without phage LHE83 was used as a control. The MOI that generated the highest phage titer within 4 h was considered the optimal MOI. Each experiment was repeated 3 times.

Stability Assay of Phage LHE83

The stability of phage LHE83 to temperatures, pH, and UV light was evaluated by the double-layer agar plate method. For the thermal-stability assay, phage LHE83 (10^8 pfu/mL) was incubated at various temperatures (40°-80°C), and samples were collected after 20, 40, and 60 min of incubation. For the pH stability assay, a phage suspension was inoculated in LB broth at different pH (3−12) at 37°C, and aliquots were collected at 1, 2, and 3 h. For the UV stability assay, a phage suspension was exposed to UV light, and samples were collected every 10 min for up to 1 h. Each experiment was repeated 3 times.

Sequencing and Genomic Analysis of Phage LHE83

The genome of phage LHE83 was sequenced on an Illumina Nextseq platform using PE150 strategies by Novogene Co. Ltd (Chaoyang District, Beijing, China). The acquired genome sequence was then annotated using the RAST server (https://rast.nmpdr.org/) and submitted to the GeneBank database (OQ561750). Furthermore, an evolutionary tree was constructed using MEGA software to analyze the genetic relationships between phage LHE83 and other related phages.

Identification of Receptor Binding Protein of Phage LHE83

According to the RAST annotation, the predicted tail fiber GP213 of phage LHE83 was compared with the RBP GP38 of phage Bp7, and the sequence features were analyzed. Then, as previously described(Chen et al., 2020), the *ORF 213* sequence was amplified from extracted phage LHE83 genomic DNA by PCR using designed primers (Table S1) to construct the recombinant plasmid pCold-*GP*213 using ClonExpress II One-step cloning Kit (Vazyme, Nanjing). The plasmid was transformed into *E. coli* BL21 and inducted by 0.1 mmol/L IPTG at 16°C for 12 h to express the recombinant protein. After ultrasonic treatment, the GP213 protein was purified by affinity chromatography. To prepare antiserum of GP213, New Zealand white rabbits were immunized 3 times with GP213 protein. The serum was collected 5 days after the final immunization and stored at - 80°C until use. To evaluate the antibody-blocking effect of GP213, 100 μL of the GP213 antiserum was mixed with an equal volume of phage LHE83 (10^4 pfu/mL), then incubated with 200 μL of *E. coli* BL21 (10^8 pfu/mL) at 37°C for 5 min. Serum collected before immunization was used as a control. The mixtures were centrifugated at 12 000 g for 5 min, and the free virions in the supernatant were counted by the double-layer agar method to quantify the phage adsorption rates. Each experiment was performed in triplicate.

Selection of Phage-Resistant Strains

Phage-resistant strains were selected through the co-cultivation of phages and host bacteria by the double-layer agar method. Briefly, phage LHE83 and *E. coli* E82 were added to the top agar layer in a ratio of 10:1 (MOI = 10) and incubated overnight at 37°C. Subsequently, individual colonies were picked and streaked on agar plates for purification through 3 generations to obtain phage-resistant strains. Phage sensitivity assays were performed on mutant strain *E. coli* E82-R5 using the double-layer agar method with phage LHE83.

Genomic Sequencing and Analysis of Phage-Resistant Mutants

Whole-genome sequencing of *E. coli* E82 and *E. coli* E82-R5 was conducted using an Illumina Nextseq platform with PE150 sequencing strategies by Novogene Co. Ltd. Then, their genome sequences were aligned using the Burrows-Wheeler-Algnment tool (**BWA**) to identify the specific locus responsible for phage resistance.

Identification of OmpA as the Receptor on E. coli *BL21*

Based on genome sequencing and analysis, the gene potentially encoding the receptor was knocked out in the *E. coli* BL21 strain using the no-scar system as described before (Reisch and Prather, 2015). In brief, the sgRNA was designed to construct plasmid pKDsg-OmpA (Table S1). Then, plasmids Cas9 and pKDsg-OmpA were transferred into *E. coli* BL21. After induction with 50 mM L-arabinose, competent cells of *E. coli* BL21 were prepared. A 140-bp DNA fragment containing both sides of the target OmpA gene-coding region, with 3 phosphorothioate bonds at the 5′ end (Table S1), was electroporated into *E. coli* BL21 competant cells. The transformed cells were then screened using 50 μg/mL kanamycin, 25 μg/mL SPEC, and 100 ng/mL aTc at 30°C. The gene knockout strain *E. coli* BL21ΔOmpA was identified by PCR. The *E. coli* BL21ΔOmpA were incubated at 37°C to eliminate the temperature-sensitive plasmid pKDsg-OmpA. Moreover, the *OmpA* gene of *E. coli* E82 was amplified to construct the recombinant plasmid pCold-OmpA. The plasmid was then transferred into *E. coli* BL21 or *E. coli* BL21ΔOmpA, and inducted with 0.1 mM IPTG at 37°C for 8 h to obtain the overexpressing strain *E. coli* BL21:OmpA or the complementation strain *E. coli* BL21ΔOmpA: OmpA. The adsorption rates of phage LHE83 on these strains were assayed using the double-layer agar method to confirm the role of OmpA. The *E. coli* BL21 wild-type strain was used as a control, and each assay was repeated 3 times.

The Synergy Assay of Phage LHE83 and SPEC in the Inhibition of E. coli *E82*

Several antibiotics were used to evaluate the synergistic effect of phage LHE83 on the *E. coli* E82 strain, including NEO, DOX, COL, AMX, ENR, and SPEC. Briefly, 100 μL various concentrations of antibiotics (0 −256 μg/mL) and phage LHE83 lysate (0−10^9 pfu/mL) were mixed in equal volume. A total of 100 μL *E. coli* E82 cells in the logarithmic growth phase were added to the mixture in 96-well plates. The plates were then incubated at 37°C for 12 h. The OD_{630} of the mixed cultures was measured every 30 min. The data were analyzed using Prism software for statistical analysis. The experiment was repeated 3 times.

ACKNOWLEDGMENTS

We gratefully acknowledge the staff from the Central Lab of Qingdao Agricultural University for their support on TEM observation. This work was supported by the National Key R&D Program of China (2023YFD1800303); the Shandong Province Key Research and Development Program (2022CXGC010606-01-05); and the Modern Agricultural Technology System Innovation Team of Shandong Province (SDAIT-27-04).

DISCLOSURES

The authors declare no conflicts of interest.

SUPPLEMENTARY MATERIALS

Supplementary material associated with this article can be found, in the online version, at doi:10.1016/j.psj.2024.103643.

REFERENCES

Aghaee, B. L., M. Khan Mirzaei, M. Y. Alikhani, A. Mojtahedi, and C. F. Maurice. 2021. Improving the inhibitory effect of phages against pseudomonas aeruginosa isolated from a burn patient using a combination of phages and antibiotics. Viruses 13:334.

Ajiboye, R. M., O. D. Solberg, B. M. Lee, E. Raphael, C. Debroy, and L. W. Riley. 2009. Global spread of mobile antimicrobial drug resistance determinants in human and animal Escherichia coli and Salmonella strains causing community-acquired infections. Clin. Infect Dis 49:365–371.

Allen, R. C., K. R. Pfrunder-Cardozo, D. Meinel, A. Egli, and A. R. Hall. 2017. Associations among antibiotic and phage resistance phenotypes in natural and clinical isolates. Mbio. 8:e01341-17.

Chaudhry, W. N., J. Concepcion-Acevedo, T. Park, S. Andleeb, J. J. Bull, and B. R. Levin. 2017. Synergy and order effects of antibiotics and phages in killing pseudomonas aeruginosa biofilms. PLoS One 12:e0168615.

Chen, P., H. Sun, H. Ren, W. Liu, G. Li, and C. Zhang. 2020. LamB, OmpC, and the core lipopolysaccharide of escherichia coli K-12 function as receptors of bacteriophage Bp7. J. Virol 94:e00325-20.

Clokie, M. R., A. D. Millard, A. V. Letarov, and S. Heaphy. 2011. Phages in nature. Bacteriophage 1:31–45.

Degroux, S., G. Effantin, R. Linares, G. Schoehn, and C. Breyton. 2023. Deciphering bacteriophage T5 host recognition mechanism and infection trigger. J. Virol 97:e0158422.

Diaz-Munoz, S. L., and B. Koskella. 2014. Bacteria-phage interactions in natural environments. Adv. Appl. Microbiol 89:135–183.

Elbreki, M., R. P. Ross, C. Hill, J. O'Mahony, O. McAuliffe, and A. Coffey. 2014. Bacteriophages and their derivatives as biotherapeutic agents in disease prevention and treatment. J. Viruses 2014:1–20.

Gao, M., C. Feng, Y. Ji, Y. Shi, W. Shi, L. Zhang, S. Liu, A. Li, X. Zhang, Q. Li, J. Lu, Q. Bao, and H. Zhang. 2022. AadA36, a novel chromosomal aminoglycoside nucleotidyltransferase from a clinical isolate of Providencia stuartii. Front. Microbiol. 13:1035651.

Gonzalez-Serrano, R., M. Dunne, R. Rosselli, A. B. Martin-Cuadrado, V. Grosboillot, L. V. Zinsli, J. J. Roda-Garcia, M. J. Loessner, and F. Rodriguez-Valera. 2020. Alteromonas myovirus V22 represents a new genus of marine bacteriophages requiring a tail fiber chaperone for host recognition. mSystems 5:e00217-20.

Gordillo Altamirano, F. L., and J. J. Barr. 2019. Phage therapy in the postantibiotic era. Clin. Microbiol. Rev 32:e00066-18.

Gordillo Altamirano, F. L., and J. J. Barr. 2021. Unlocking the next generation of phage therapy: the key is in the receptors. Curr Opin Biotechnol 68:115–123.

Hampton, H. G., B. N. J. Watson, and P. C. Fineran. 2020. The arms race between bacteria and their phage foes. Nature 577:327–336.

Hoyland-Kroghsbo, N. M., R. B. Maerkedahl, and S. L. Svenningsen. 2013. A quorum-sensing-induced bacteriophage defense mechanism. mBio 4:e00362-12.

Jin, Y., W. Li, H. Zhang, X. Ba, Z. Li, and J. Zhou. 2023. The post-antibiotic era: a new dawn for bacteriophages. Biology (Basel) 12:681.

Labrie, S. J., J. E. Samson, and S. Moineau. 2010. Bacteriophage resistance mechanisms. Nat. Rev. Microbiol 8:317–327.

Lavelle, K., A. Goulet, B. McDonnell, S. Spinelli, D. van Sinderen, J. Mahony, and C. Cambillau. 2020. Revisiting the host adhesion determinants of Streptococcus thermophilus siphophages. Microb. Biotechnol 13:1765–1779.

Li, G., M. Shen, Y. Yang, S. Le, M. Li, J. Wang, Y. Zhao, Y. Tan, F. Hu, and S. Lu. 2018. Adaptation of pseudomonas aeruginosa to

phage PaP1 predation via O-antigen polymerase mutation. Front. Microbiol 9:1170.
Li, X., Y. He, Z. Wang, J. Wei, T. Hu, J. Si, G. Tao, L. Zhang, L. Xie, A. E. Abdalla, G. Wang, Y. Li, and T. Teng. 2021. A combination therapy of phages and antibiotics: two is better than one. Int. J. Biol. Sci 17:3573–3582.
Monroe, S., and R. Polk. 2000. Antimicrobial use and bacterial resistance. Curr. Opin. Microbiol 3:496–501.
North, O. I., and E. D. Brown. 2021. Phage-antibiotic combinations: a promising approach to constrain resistance evolution in bacteria. Ann. N Y Acad. Sci 1496:23–34.
Oechslin, F. 2018. Resistance development to bacteriophages occurring during bacteriophage therapy. Viruses 10:351.
Ofir, G., and R. Sorek. 2018. Contemporary phage biology: from classic models to new insights. Cell 172:1260–1270.
Reisch, C. R., and K. L. Prather. 2015. The no-SCAR (Scarless Cas9 assisted recombineering) system for genome editing in *Escherichia coli*. Sci Rep 5:15096.
Shen, M., H. Zhang, W. Shen, Z. Zou, S. Lu, G. Li, X. He, M. Agnello, W. Shi, F. Hu, and S. Le. 2018. Pseudomonas aeruginosa MutL promotes large chromosomal deletions through non-homologous end joining to prevent bacteriophage predation. Nucleic Acids Res 46:4505–4514.
Simon, K., W. Pier, A. Kruttgen, and H. P. Horz. 2021. Synergy between Phage Sb-1 and oxacillin against methicillin-resistant *Staphylococcus aureus*. Antibiotics (Basel) 10:849.
Smani, Y., A. Fabrega, I. Roca, V. Sanchez-Encinales, J. Vila, and J. Pachon. 2014. Role of OmpA in the multidrug resistance phenotype of Acinetobacter baumannii. Antimicrob. Agents Chemother 58:1806–1808.
Strathdee, S. A., G. F. Hatfull, V. K. Mutalik, and R. T. Schooley. 2023. Phage therapy: from biological mechanisms to future directions. Cell 186:17–31.
Sui, B., X. Qi, X. Wang, H. Ren, W. Liu, and C. Zhang. 2021. Characterization of a novel bacteriophage swi2 harboring two lysins can naturally lyse *Escherichia coli*. Front. Microbiol 12:670799.
Tan, D., S. L. Svenningsen, and M. Middelboe. 2015. Quorum sensing determines the choice of antiphage defense strategy in vibrio anguillarum. mBio 6:e00627.
Taslem Mourosi, J., A. Awe, W. Guo, H. Batra, H. Ganesh, X. Wu, and J. Zhu. 2022. Understanding bacteriophage tail fiber interaction with host surface receptor: the key "blueprint" for reprogramming phage host range. Int. J. Mol. Sci 23:12146.
Torres-Barcelo, C., J. Gurney, C. Gougat-Barbera, M. Vasse, and M. E. Hochberg. 2018. Transient negative effects of antibiotics on phages do not jeopardise the advantages of combination therapies. FEMS Microbiol. Ecol 94:10.
Trojet, S. N., A. Caumont-Sarcos, E. Perrody, A. M. Comeau, and H. M. Krisch. 2011. The gp38 adhesins of the T4 superfamily: a complex modular determinant of the phage's host specificity. Genome Biol. Evol 3:674–686.
von Baum, H., and R. Marre. 2005. Antimicrobial resistance of *Escherichia coli* and therapeutic implications. Int. J. Med. Microbiol 295:503–511.
Wang, X., B. Loh, F. Gordillo Altamirano, Y. Yu, X. Hua, and S. Leptihn. 2021. Colistin-phage combinations decrease antibiotic resistance in Acinetobacter baumannii via changes in envelope architecture. Emerg. Microbes. Infect 10:2205–2219.
Zhang, C., W. Li, W. Liu, L. Zou, C. Yan, K. Lu, and H. Ren. 2013. T4-like phage Bp7, a potential antimicrobial agent for controlling drug-resistant Escherichia coli in chickens. Appl. Environ. Microbiol 79:5559–5565.
Zhang, Z., C. E. Morgan, M. Cui, and E. W. Yu. 2023. Cryo-EM structures of AcrD illuminate a mechanism for capturing aminoglycosides from its central cavity. mBio 14:e0338322.
Zuo, P., P. Yu, and P. J. J. Alvarez. 2021. Aminoglycosides antagonize bacteriophage proliferation, attenuating phage suppression of bacterial growth, biofilm formation, and antibiotic resistance. Appl. Environ. Microbiol 87:e0046821.